J Mater Sci: Mater Med (2008) 19:3105–3114
DOI 10.1007/s10856-008-3446-x

Osteoblast behaviour on in situ photopolymerizable three-dimensional scaffolds based on D,L-lactide and ε-caprolactone: influence of pore volume, pore size and pore shape

Heidi A. Declercq · Tomasz L. Gorski · Etienne H. Schacht · Maria J. Cornelissen

Received: 5 September 2006 / Accepted: 24 March 2008 / Published online: 15 April 2008

Abstract Bone marrow cells were cultured on in situ photopolymerizable scaffolds based on D,L-lactide and ε-caprolactone. The influence of pore volume, size and shape were evaluated. Bone formation was demonstrated by ALP activity, osteocalcin secretion and histological analysis. TEM at the polymer interface revealed osteoblasts which secreted an extracellular matrix containing matrix vesicles loaded with apatite. Cellular infiltration was possible for scaffolds with a porosity of 70 and gelatin particle size of 250–355 μm. Scaffolds with a porosity less than 70 had the tendency to form a polymer top layer. Although increasing the gelatin particle size to 355–500 μm, leads to infiltration even in scaffolds with a porosity of 60. No infiltration was possible in scaffolds with sodium chloride as porogen. On the contrary, sucrose and gelatin leads to better interconnected scaffolds at the same porosity. Hence, spherical gelatin particles are suitable to use as porogen in photopolymerizable scaffolds.

1 Introduction

The shortcomings of auto- and allografting have inspired the development of tissue engineering. Tissue engineering generally requires the use of a porous, bioresorbable scaffold, which serves as a three-dimensional (3-D) template for initial cell attachment and subsequent tissue formation, both in vitro and in vivo [1]. The increasing popularity of arthroscopic procedures in orthopaedics and the requirement to bridge irregular bone defects resulted in great interest in fixation materials (both ceramic and polymeric-based) that are injectable, in situ forming and biodegradable [2]. Ideally, an (injectable, in situ forming) 3-D scaffold should have the following characteristics: (1) biocompatible, (2) highly porous with an interconnected pore network, (3) biodegradable to promote new tissue formation and vascularization, (4) suitable surface chemistry to allow cell attachment and differentiation, (5) mechanical properties that match those of the tissues at the site of implantation and (6) contain osteoinductive factors [1, 2]. To achieve the above mentioned characteristics, moldable polymers (degradation times and mechanical properties can be tailored) can be mixed with calcium phosphate cements (to improve the mechanical properties) and pore forming particulates (e.g. gelatin), injected and subsequently crosslinked in situ.

In situ photopolymerizable 3-D scaffolds based on D,L-lactide and ε-caprolactone combined with leachable compounds to create porosity are promising biomaterials, but should be tested in an in vitro model prior to in vivo testing.

In this regard, the in vitro differentiation of bone marrow derived osteoblastic cells on in situ photopolymerized 3-D scaffolds based on D,L-lactide and ε-caprolactone will be evaluated concerning porosity. Scaffolds with the highest interconnectivity and the lowest possible pore volume (to minimize the loss in mechanical strength)

H. A. Declercq · M. J. Cornelissen (✉)
Department of Anatomy, Embryology, Histology and Medical Physics, Ghent University, De Pintelaan 185 (6B3), 9000 Ghent, Belgium
e-mail: ria.cornelissen@Ugent.be

H. A. Declercq
e-mail: Heidi.Declercq@Ugent.be

T. L. Gorski · E. H. Schacht
Polymer Material Research Group, Ghent University, Krijgslaan 281 (S4), 9000 Ghent, Belgium

should be obtained. For this reason, different porogens having different sizes, shape and volume will be compared in this study.

The efficiency of gelatin and sucrose, acceptable as a porogen for in vivo applications, as pore forming particulates will be compared to the often used salt-leaching technique. The importance of porosity and interconnectivity will be related to the properties of different pore forming particulates (gelatin, sucrose, sodium chloride) with regard to pore size, pore volume and pore shape.

The following questions related to the in situ formed 3-D scaffolds will be answered: (1) is in vitro bone formation possible in in situ photopolymerized 3-D scaffolds based on D,L-lactide and ε-caprolacton? (2) can gelatin, a porogen suitable for in vivo application, be used as a pore forming particulate? (3) what is the minimum pore size and pore volume to obtain the highest interconnectivity?

2 Materials and methods

2.1 Materials

α-MEM supplemented with nucleotides (α-MEM DNA/RNA) (Cat No. 22571-020), fetal bovine serum (FBS heat inactivated, E.C. approved), L-glutamine, penicillin–streptomycin (10,000 U/ml–10,000 μg/ml) and Fungizone® were purchased from Gibco BRL (Life Technologies, Merelbeke, Belgium). L-ascorbic acid 2-phosphate, β-glycerophosphate, dexamethasone (Cat No. D-2915) and 1,25 dihydroxyvitamin D_3 (Cat No. D-1530-10UG), tetracycline (T-7660) and MTT (thiazolyl blue tetrazolium (M-5655) were supplemented from Sigma (Sigma-Aldrich NV/SA, Bornem, Belgium). Tissue culture dishes were purchased from Greiner (Frickenhausen, Wemmel, Belgium). Gelatin was from Gelatines Rousselot®.

p-Nitrophenylphosphate, *p*-nitrophenol and glycine were purchased from ICN Biomedicals, Inc. (Asse-Relegem, Belgium). The protein assay kit and bovine gamma globulin standard was supplemented from Bio-Rad Laboratories (Nazareth-Eke, Belgium). UltraClear and MountingClear were obtained from J.T. Baker (Klinipath, Geel, Belgium). The rat osteocalcin EIA kit BT 490 was purchased from Biomedical Technologies, Inc. (Sanbio, Uden, The Netherlands).

2.2 Scaffold preparation

2.2.1 Synthesis of methacrylate-endcapped poly(D,L-lactide-co-ε-caprolactone) oligomer

Linear, telechelic poly(D,L-lactide-co-ε-caprolactone) with hydroxyl groups at the termini was synthesized by the ring-opening polymerization of D,L-lactide (LA) and ε-caprolactone (CL) in the presence of 1,6-hexanediol (HXD) as an initiator and zinc acetate as a catalyst. Polymerization was performed in bulk at 140°C for 48 h and on a 15 g scale. A glass tube was silanized with dichlorodimethylsilane, dried in an oven, and cooled in a dessicator. A typical experimental procedure was as follows: the glass tube was charged with predetermined amounts of comonomers (LA/CL molar ratio 50/50), the initiator, and the catalyst. The target number average molecular weight was 2,700 $gmol^{-1}$. The tube was degassed three times, sealed, and placed in a constant-temperature oven. Polymerization was terminated by cooling the tube in a refrigerator.

In the second step, the poly(D,L-lactide-co-ε-caprolactone) diol was endcapped using excess of methacryloyl chloride (twofolds excess to the total number of hydroxyl groups derived from the oligomer) in the presence of triethylamine (1.5 molar excess to the amount of methacryloyl chloride) in methylene chloride (2:1 volume ratio) to give the corresponding methacrylate-endcapped oligomer. The esterification proceeded at room temperature for 24 h. The triethylamine hydrochloride produced from the reaction was removed by filtration and the remaining solution was concentrated and stored in a freezer for 1 h, and again a white solid was filtrated. Finally, the remaining solution was dialysed (Spectra/Por® Membrane, MWCO: 1000) in dry acetone for 2 days. The yield was 62%.

2.2.2 Scaffold preparation

The methacrylate-endcapped copolymers can be converted into a solid, 3-D polymer network by visible-light irradiation in the presence of D,L-camphorquinone/ethyl 4-dimethylaminobenzoate initiator system. By adding leachable particulates (porogens), a porous 3-D network can be obtained [3–7].

The porogens, respectively gelatin, sucrose and sodium chloride were sieved with ASTM E11-70 standard testing sieves with openings of 250, 355 and 500 μm, placed on the Retsch AS 200 sieved shaker until particulates with a defined particle size (250–355 and 355–500 μm) were obtained.

Hydroxy ethyl methacrylate (HEMA) (15 wt%) was added to the catalyst (0.6 wt% D,L-camphorquinone and 0.7 wt% ethyl 4-dimethylaminobenzoate) until dissolved. The HEMA/catalyst solution followed by the porogen is added to the viscous prepolymer and mixed thoroughly. The viscous paste is then brought into cylindrical Teflon molds (diameter 5 mm, height 1 mm) and the prepolymer is photopolymerized for 20 s at one side with the dental lamp curing unit (500 mW/cm^2) (3M Unitek™, Ortholux™ XT) (3M Dental Products). After polymerization, the scaffolds are removed from the mold and immersed in

distilled water (37°C, bench shaker, 55 rpm) for a period of 72 h (to leach out the porogen). The scaffolds were dried under reduced pressure in a vacuum oven (3 days, room temperature) and sterilized by ethylene oxide (12 h, 60°C, 48 h aerated) [6–8].

Scaffolds with apparent porosity of 50 and 60 were prepared with gelatin as porogen and particle size (250–355 and 355–500 μm). Scaffolds with apparent porosity of 70 were prepared with respectively gelatin, sucrose and sodium chloride as porogens with particle size 250–355 μm [8].

2.3 Scaffold characterization

2.3.1 Porosity

To determine the density of the solid polymeric material and the sucrose particles, the measurements using pycnometry were performed in triplicate. The density of polymeric material is 1.13 g/cm^3. The density of sucrose, sodium chloride and gelatin particles is respectively 1.71, 2.16 and 0.97 g/cm^3 [5, 9].

The porosities of the porous scaffolds were calculated from the theoretical apparent densities of the scaffolds using the following equation described by Mikos et al.: $\varepsilon = \left[w_s/d_s\right]/\left[(1-w_s)/d_p + w_s/d_s\right]$ where ε is the theoretical prediction of an apparent porosity, w_s is the porogen weight fraction, d_s and d_p is the density of respectively the porogen and the polymer [10].

2.3.2 Scanning electron microscopy

The scaffolds were sputter-coated with phalladium-gold before being examined in a FEI Quanta 200G electron microscope operating at a voltage of 20 kV [8].

2.4 Cell culture and scaffold/cell culturing

2.4.1 Isolation and culture of bone marrow derived cells

Bone marrow cells were obtained from the tibiae and femora of young (6 weeks old) adult male Wistar rats. Skin, soft connective tissue and periosteum were removed. Tibiae and femora were washed and the diaphyses were cut free of epiphyseal cartilage. The bone marrow was flushed out repeatedly with MEM Alpha medium (containing 10 vol% fetal bovine serum, 0.5 vol% penicillin–streptomycin, 1 vol% Fungizone®), supplemented with 100 μM L-ascorbic acid 2-phosphate and 10 nM dexamethasone and centrifuged (10 min, 1,000 rpm) [11]. The cell pellet was resuspended and seeded in T75 tissue culture dishes. After 24 h, the medium was changed to remove nonadherent cells. The cells were cultured until confluence (5% CO_2/95% air, 37°C). After 7 days of primary culture, the cells were detached using trypsin/EDTA, concentrated by centrifugation at 1,000 rpm for 10 min and resuspended in complete MEM Alpha medium.

2.4.2 Cell seeding and growth on porous scaffolds

Before cell seeding, the scaffolds were immersed in serum-free MEM Alpha medium in Eppendorf tubes. Air was removed from their pores by generating vacuum with a 20 ml syringe equipped with an 18-gauge needle. The scaffolds were left in medium on a bench shaker (37°C, 55 rpm). After 24 h, the scaffolds were placed into 96-well tissue culture dishes (for suspension culture).

The scaffolds were seeded with 700,000 respectively 435,000 rat bone marrow cells/90 μl/scaffold (3.6×10^6 cells/cm^2 (high seeding density) respectively 2.2×10^6 cells/cm^2 (low seeding density)) and incubated for 4 h. Then 160 μl medium was added to each well. The seeded scaffolds were further incubated overnight to allow for cell attachment [12].

After 24 h, scaffolds (seeded with 435,000 cells) were evaluated for their seeding efficiency by replacing the medium by MTT containing medium (0.5 mg/ml). After 4 h incubation, the MTT containing solution was withdrawn and 0.5 ml of 1% Triton X-100 in isopropanol/0.4 N HCl was added. The formazan was dissolved by shaking at 37°C for 30 min. The absorbance of 300 μl solution was measured at 580 nm (Universal Microplate Reader EL 800, BIO-TEK instruments Inc.) and the viability was calculated as percentage of the control (tissue culture dish). Each scaffold was tested in triplicate.

Scaffolds for continuous growth were placed on a needle (3 scaffolds/needle) in a 5 ml spinner flask. Three milliliter culture medium supplemented with 10 mM β-glycerophosphate was added and the cell/scaffold constructs were cultured for 21 days on a bench shaker at a constant rate of 55 rpm (5% CO_2/95% air, 37°C). Each scaffold was tested in three independent experiments in triplicate.

2.5 Analysis

2.5.1 Alkaline phosphatase activity and protein content

Cell/scaffold constructs were lysed into 0.5 ml of a Triton X-100 containing Tris HCl buffer, homogenized by two freeze-and-thaw cyclic and sonicated on ice for 3 × 10 s (40 mA) (Vibra Cell™ SONICS (ANALIS)). Fifty microliter samples were added to 50 μl *p*-nitrophenyl-phosphate (4.34 mM) in glycine buffer (pH 10.3) and incubated (37°C, 30 min) on a bench shaker. 50 μl NaOH (1 M) was added, the absorbance was measured at 405 nm and the enzyme activity was calculated according to

p-nitrophenol standards. Alkaline phosphatase activity was expressed as mM *p*-nitrophenol/scaffold.

Total protein content was determined with the Bradford method, read at 595 nm and calculated according to bovine gamma globulin standards.

Scaffolds of three independent experiments in duplicate were analyzed.

2.5.2 Osteocalcin

Forty-eight hours prior to assaying (21 days), each scaffold was placed into 3 ml serum-free osteogenic medium containing 10^{-9} M 1,25-dihydroxyvitamin D_3 in 12 well tissue culture dishes. After 48 h, the medium was harvested and frozen (−20°C). At the time of analysis, the medium was thawed and osteocalcin was measured at 450 nm by an enzyme immuno assay according to the company's instructions.

2.5.3 Histology

Four hours prior to fixation, 10 μg tetracycline/ml was added to the osteogenic medium. Scaffolds were rinsed with Ringer solution, fixed with 4% phosphate (10 mM) buffered formaldehyde (pH 6.9) (4°C, 24 h), dehydrated in a graded alcohol series (UltraClear is used instead of toluene because toluene dissolves the polymer) and embedded in paraffin. Sections of 5–7 μm were made and stained with hematoxylin and eosin, Masson's Trichrome, von Kossa and mounted with MountingClear. Tetracycline incorporation, indicative for calcium depositions, was evaluated in unstained sections by fluorescence microscopy.

2.5.4 Transmission electron microscopy

Scaffolds were fixed (4°C, 1 h) in 1% glutaraldehyde buffered with 0.1 M sodium cacodylate (pH 7.2), washed in the same buffer, postfixed with osmium tetroxide, dehydrated in graded concentration of alcohol and embedded in epoxy-resin. Thin sections (60 nm) were cut with a diamand knife, mounted on cupper grids, stained with uranyl acetate and lead citrate and examined using a JEOL 1200 EX II transmission electron microscope operating at 80 KeV.

3 Results

Scaffolds seeded with rat bone marrow cells were cultured dynamically. After 21 days, the alkaline phosphatase activity and osteocalcin secretion were evaluated as markers representative for differentiated osteoblast-like cells present on the scaffold. Cellular infiltration was studied by histological analysis.

3.1 Influence of porosity (pore volume)

LA/CL scaffolds with apparent porosities of 50, 60 and 70 with pore sizes of 250–355 μm (gelatin as porogen) were prepared and compared with regard to bone formation and cellular infiltration.

Scaffolds with apparent porosity of 60 have a limited ALP activity, osteocalcin secretion and negligible protein content in comparison to scaffolds with apparent porosity of 70 (Fig. 1a).

Histological analysis of LA/CL scaffolds with a porosity of 50 and 60 showed empty scaffolds (Fig. 2a) or a layer of osteoblast-like cells, but detached from the scaffold (Fig. 2b). The cells were able to attach to the polymer scaffold as shown by the seeding efficiency, 53.3 ± 13% of the total number of cells adhered to LA/CL scaffolds after 24 h. However, it seems that the cells were not able to infiltrate into the scaffold and finally detached as demonstrated by the negligible protein content.

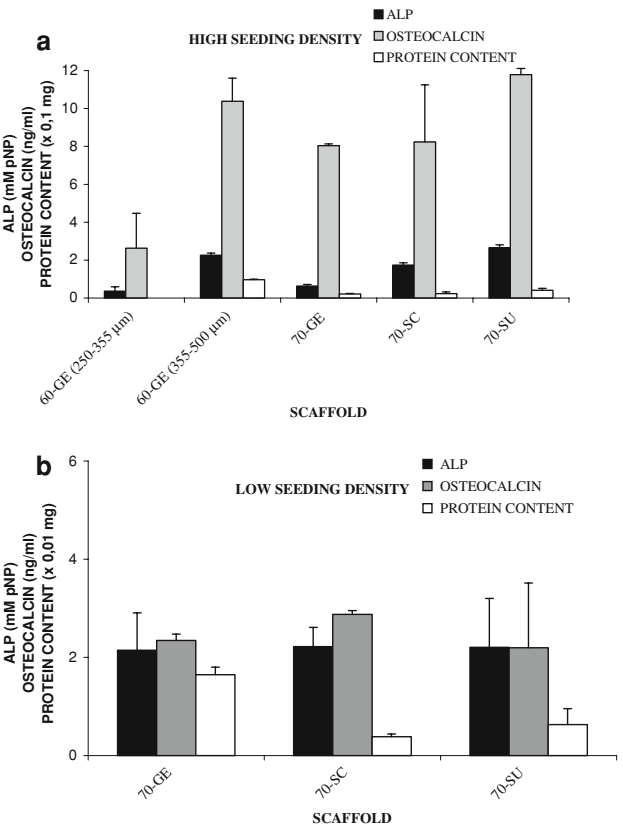

Fig. 1 Differentiation of rat bone marrow cells cultured for 21 days on LA/CL scaffolds prepared with different apparent porosity [60 and 70], pore size (250–355 and 355–500 μm) and porogens (gelatin, sucrose, sodium chloride) (pore shape). ALP activity, osteocalcin and protein content was expressed as respectively mM *p*-nitrophenol/scaffold, ng/ml and mg × 10^{-1}/scaffold. Mean and SD, n = 3. (**a**) Scaffolds seeded with 700,000 cells/scaffold (high seeding density). (**b**) Scaffolds seeded with 435,000 cells/scaffold (low seeding density)

At the edge of the scaffold, a polymer top layer can be detected (Fig. 2a, b). This was confirmed by SEM which showed that scaffolds with an apparent porosity of 60 or less, have a tendency to form a polymer top layer (Fig. 3a). Hence, cells are not able to infiltrate into a LA/CL scaffold with an apparent porosity of 50 and 60 with pore sizes of 250–355 μm (obtained with gelatine as porogen).

Scaffolds with apparent porosity of 70 (gelatin as porogen) have high ALP activity and osteocalcin secretion for high as well as low seeding densities (Fig. 1a, b). As seen in cross-sections, no top layer is formed and the cells can infiltrate into the scaffold (Fig. 4a, d). The absence of a top layer is confirmed by SEM (Fig. 3b).

Transmission electron micrographs at the polymer/bone interface showed osteoblast-like cells which secreted an abundant collagen I containing extracellular matrix (Fig. 5a, c). Among the collagen I fibers, matrix vesicles loaded with bone apatite crystals can be observed (Fig. 5b). Calcium phosphate deposits can be associated at the polymer edges (Fig. 5c). A polymer wall can be seen in Fig. 5d.

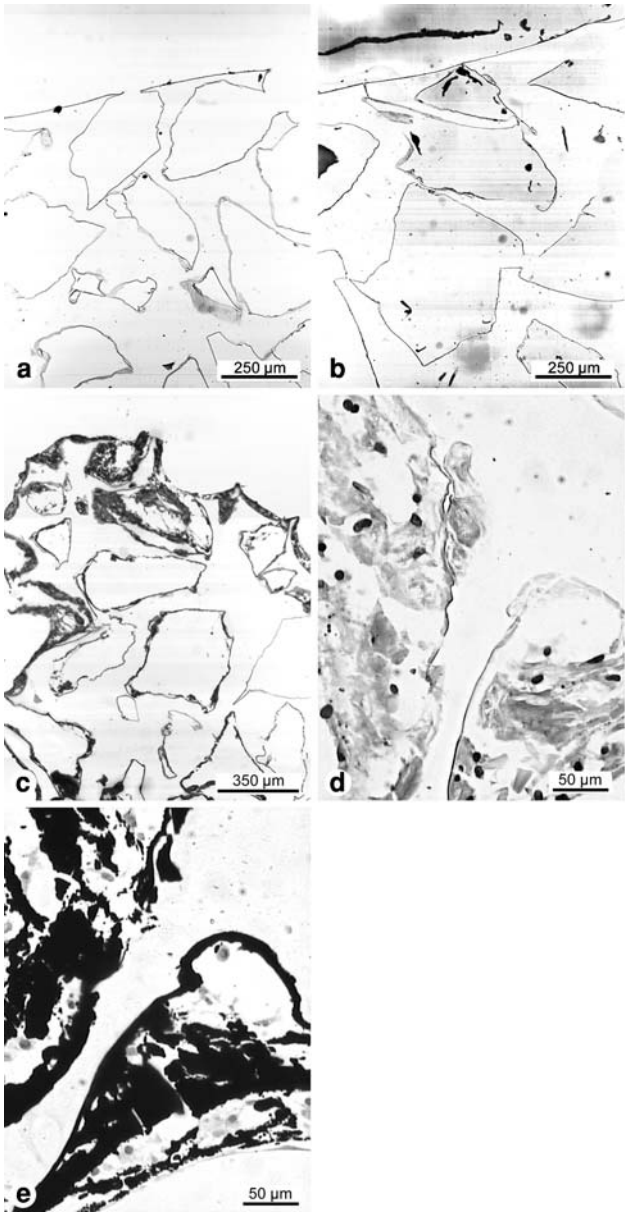

Fig. 2 Cross-sections of porous LA/CL scaffolds. (**a**) [50] Pore size 250–355 μm. A polymer top layer is seen on top of the scaffold. (**b**) [60] Pore size 250–355 μm. A layer of detached cells at the edge of the scaffolds. (**c**) [60] Pore size 355–500 μm. Bone formation and bone ingrowth at the edges. H&E stain. (**d**) [60] Pore size 355–500 μm. TM stain. (**e**) [60] Pore size 355–500 μm. von Kossa stain

3.2 Influence of pore size

As is described above, LA/CL scaffolds with apparent porosity of 60 (gelatin particle size 250–355 μm) have a limited ALP activity, osteocalcin secretion and negligible protein content.

Scaffolds with apparent porosity of 60 but with an increased particle size (355–500 μm) have high ALP activity, osteocalcin secretion and protein content (Fig. 1a). Bone formation can be detected on the scaffold (Fig. 2c). An abundant extracellular matrix with calcium phosphate deposits has been formed on the polymer walls as shown by Masson's Trichrome (Fig. 2d) and von Kossa (Fig. 2e) staining. Increasing the gelatin particle size to 355–500 μm leads to scaffolds where the top layer is not formed (Fig. 2c). Nevertheless, increasing the pore size to 355–500 μm for LA/CL scaffolds with apparent porosity of 50 did not decrease the tendency to form a polymer top layer. Hence, after a 21 days culture period, cells detached from the scaffold (data not shown).

3.3 Influence of pore shape

LA/CL scaffolds with an apparent porosity of 70 and pore sizes of 250–355 μm were prepared. The influence of pore shape on the differentiation and cellular infiltration was compared. Different pore shapes were obtained by preparing the scaffolds with the respectively porogen gelatin, sucrose and sodium chloride.

3.3.1 Bone formation

All LA/CL scaffolds, independent of porogen used, had a high ALP activity and high osteocalcin secretion for both high (Fig. 1a) and low seeding density (Fig. 1b).

Cross-sections showed nice bone formation following the contours of the polymer walls. Masson's Trichrome (Fig. 4a, c, b′) and H&E (Fig. 4b) staining showed a typical morphology of cuboidal osteoblasts which secreted an extracellular matrix. Calcium phosphate deposits can be

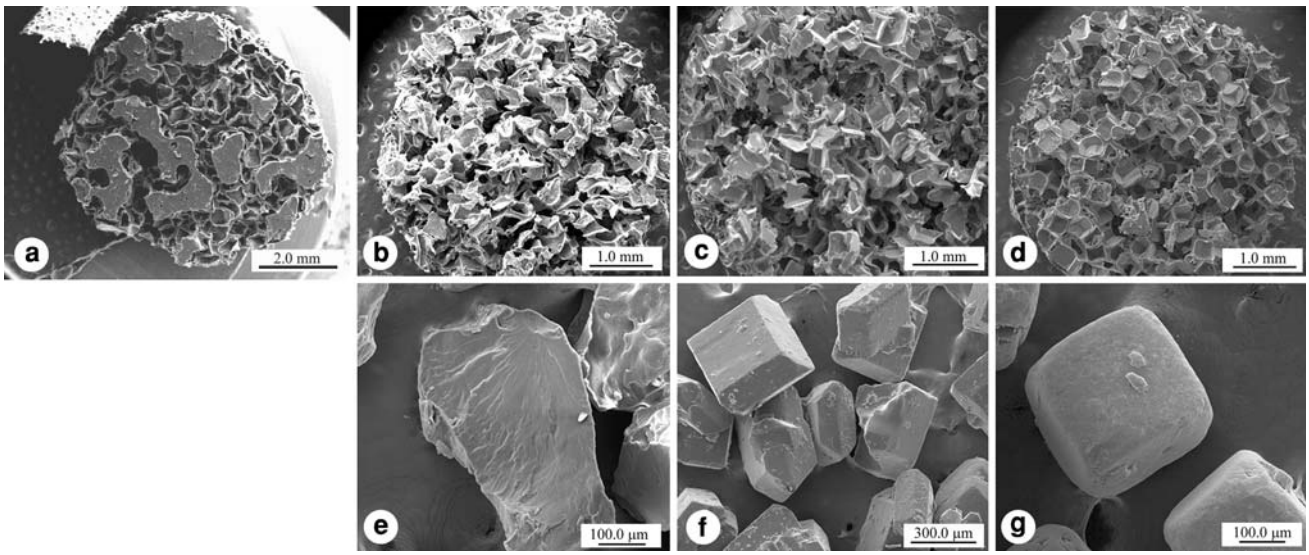

Fig. 3 SEM. (**a**) LA/CL [60] scaffold. A polymer top layer is formed. (**b**) LA/CL [70] porogen: gelatin (250–355 µm). (**c**) LA/CL [70] porogen: sucrose (250–355 µm). (**d**) LA/CL [70] porogen: sodium chloride (250–355 µm). Porogen gelatin (**e**), sucrose (**f**) and sodium chloride (**g**)

detected in the ECM as is shown by von Kossa staining (Fig. 4d, e, f).

3.3.2 Cellular infiltration

Cellular infiltration can be observed in LA/CL scaffolds prepared with porogens gelatin (Fig. 4a, d) and sucrose (Fig. 4b, e) as shown by Masson's Trichrome and von Kossa staining. For LA/CL scaffolds prepared with sodium chloride as porogen, no bone ingrowth or cellular infiltration could be observed. The rat bone marrow cells differentiated and formed new bone at the edge of the scaffold.

These results were confirmed by SEM. No interconnectivity can be observed in scaffolds with sodium chloride as porogen as shown by SEM (Fig. 3d). Sucrose as porogen leads to better interconnected pores (Fig. 3c) than sodium chloride. The best interconnectivity can be obtained with gelatin (Fig. 3b) [8]. SEM of the porogens showed that sodium chloride particles had a cuboidal shape (Fig. 3g), sucrose particles are also cuboidal but more irregularities can be observed (Fig. 3f) whereas gelatin particles have a spherical shape and are very irregular (Fig. 3e).

Although scaffolds prepared with porogen gelatin and sucrose have an interconnected pore morphology, osseous tissue is only formed at the edges of the polymer scaffolds.

4 Discussion

In the last decade, bone formation on 3-D scaffolds based on a diversity of polymers ranging from biopolymers (hyaluronic acid, chitosan, collagen) [13, 14] to synthetic polymers was often studied. Among the synthetic scaffolds, polyesters of D,L-lactide, glycolide (poly(D,L-lactide-co-glycolide) PLGA) and ε-caprolactone [1, 15–18] were intensely studied as they are approved by the Food and Drug Administration.

Characterization of these scaffolds includes descriptions of pore volume (porosity), the average pore size, pore shape, pore interconnectivity, pore roughness and pore throat size [19]. These characteristics are required for migration of cells, transport of nutrients and waste products and for cell spreading and differentiation.

However, another characteristic, making materials promising for bone tissue engineering, is the possibility to crosslink them in situ, resulting in bridging irregular defects.

Studies concerning injectable, photopolymerizable scaffolds are limited. In the literature, scaffolds are described based on lactic acid, poly(anhydrides) and poly(propylene fumarate) [2, 20–21]. In our group, a variety of in situ, photopolymerizable 3-D scaffolds were synthesized with variables of polymer type (lactide, glycolide, ε-caprolactone, trimethylene carbonate...), copolymer ratio and initiator systems. These scaffolds were compared regarding to degradation time, mechanical strength and biocompatibility [6–8, 12]. Ideally, the polymer scaffold should degrade at a rate equal to the rate of tissue ingrowth, allowing for maintenance of the scaffold structure and mechanical support during the early stages of tissue formation [22]. Our scaffolds based on P–$LA_{50}CL_{50}$–$HXD_{20/1}$–Bismethacrylate (with a porosity of 50) degrades very slowly, with $t_{1/2}$ = 135 days. These scaffolds also showed good results concerning the toxicity according to the ISO norms.

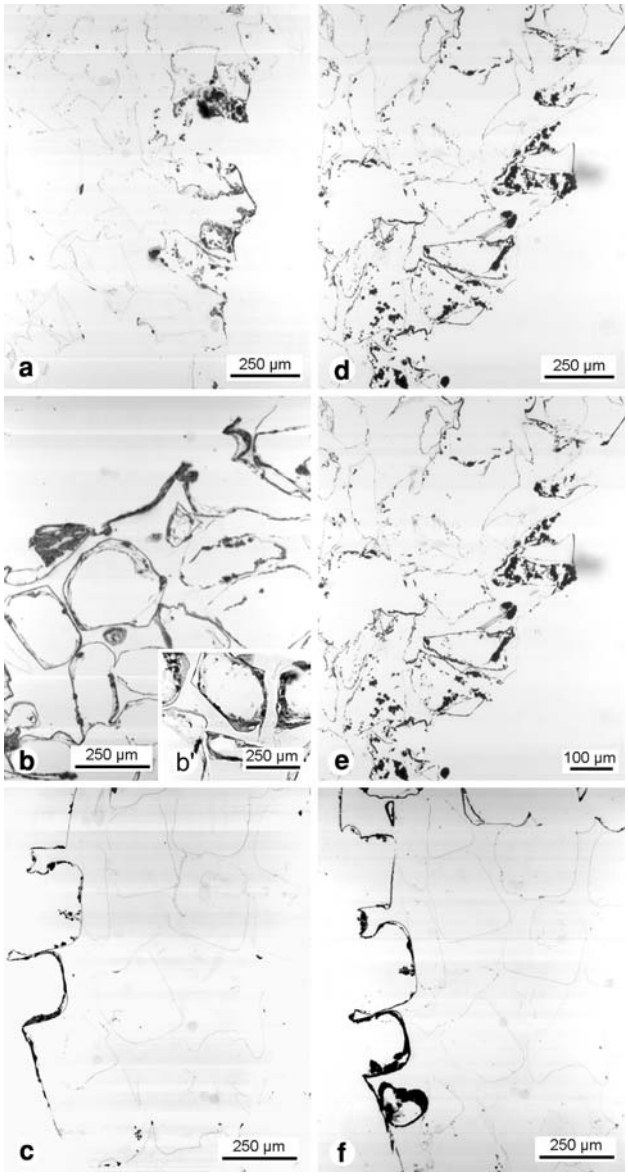

Fig. 4 Cross-sections of LA/CL scaffolds with apparent porosity of 70. (**a**, **d**) Porogen gelatin; (**b**, **e**) porogen sucrose; (**c**, **f**) porogen sodium chloride; TM stain (**a**, **c**, **b′**). von Kossa stain (**d**, **e**, **f**); H&E stain (**b**)

In the present paper, we describe physical characteristics of this LA/CL based scaffold with different pore volumes (50, 60 and 70), pore sizes (250–355 and 355–500 µm) and pore shapes obtained by gelatin, sucrose or sodium chloride leaching in correlation with the behaviour of osteoblast-like cells derived from rat bone marrow. Parameters as cell adhesion, infiltration and differentiation are evaluated.

Although cell adhesion on scaffolds based on caprolactone is described, the surface chemistry is rather hydrophobic [1, 17]. For our selected LA/CL scaffolds, with a copolymer ratio of 50/50, the seeding efficiency (or cellular adhesion) reaches an acceptable value in comparison to tissue culture dishes. Comparable seeding efficiencies were described by Ishaug et al. on PLGA scaffolds [15].

Rat bone marrow derived cells were able to attach and differentiate on these 3-D scaffolds based on LA/CL. After three weeks, the cells expressed high alkaline phosphatase activity, secreted osteocalcin and were able to mineralize the extracellular matrix. Bone formation as demonstrated by ALP activity, osteocalcin secretion and histological analysis was also observed in scaffolds based on pure caprolactone, LA, PLGA, but was not yet described for in situ forming scaffolds based on LA and CL [16, 17].

Structurally, the polymer scaffold must initially possess porosity and pore size distribution that is sufficient for cellular infiltration as well as the transport of nutrients into and cellular waste products out of the scaffold. It must be noticed that an initial high porosity (and interconnectivity) often leads to a decrease of the mechanical properties of the implant material. By comparing our scaffolds varying in pore volume (50, 60 and 70) and pore size (250–355 and 355–500 µm) obtained by gelatin leaching, the following results were obtained. LA/CL scaffolds with a porosity of 50, independent of pore size, were not suitable to allow cellular infiltration as a polymer top layer was formed. Cellular infiltration into LA/CL scaffolds with a porosity of 60 was dependent on pore size. Infiltration was possible in scaffolds where the pore size was increased to 355–500 µm. Scaffolds with apparent porosity of 70 (pore size 250–355 µm) allowed cellular infiltration. As this LA/CL scaffold degrades very slowly, the maximum pore volume should be chosen, together with the lowest risk of a polymer top layer. Other groups often describe cellular infiltration into preformed 3-D scaffolds mostly obtained by solvent casting and the salt-leaching technique. However, these scaffolds often have porosities exceeding 80% and are casted into large molds and then cut to the correct size for in vitro experiments. Consequently, there will be no top layer on the scaffolds. Hence, bone cells can easily infiltrate into the scaffold [17, 23].

Our scaffolds had good bone formation and cellular ingrowth, dependent on pore volume, for both scaffolds with pore sizes of 250–355 and 355–500 µm. The pore size does not influence osteoblast differentiation, as also described by Ishaug-Riley et al. [16]. In studies using ceramic materials for bone growth, an optimum pore size of 200–400 µm had been observed in vivo. It also has been suggested that the pore-size range of 200–400 µm is preferred by osteoblasts because it provides the optimum compression and tension on the osteoblasts mechanoreceptors [15].

In the present paper, different porogens like gelatin, sucrose and sodium chloride were compared. The particulate leaching technique is most often performed with

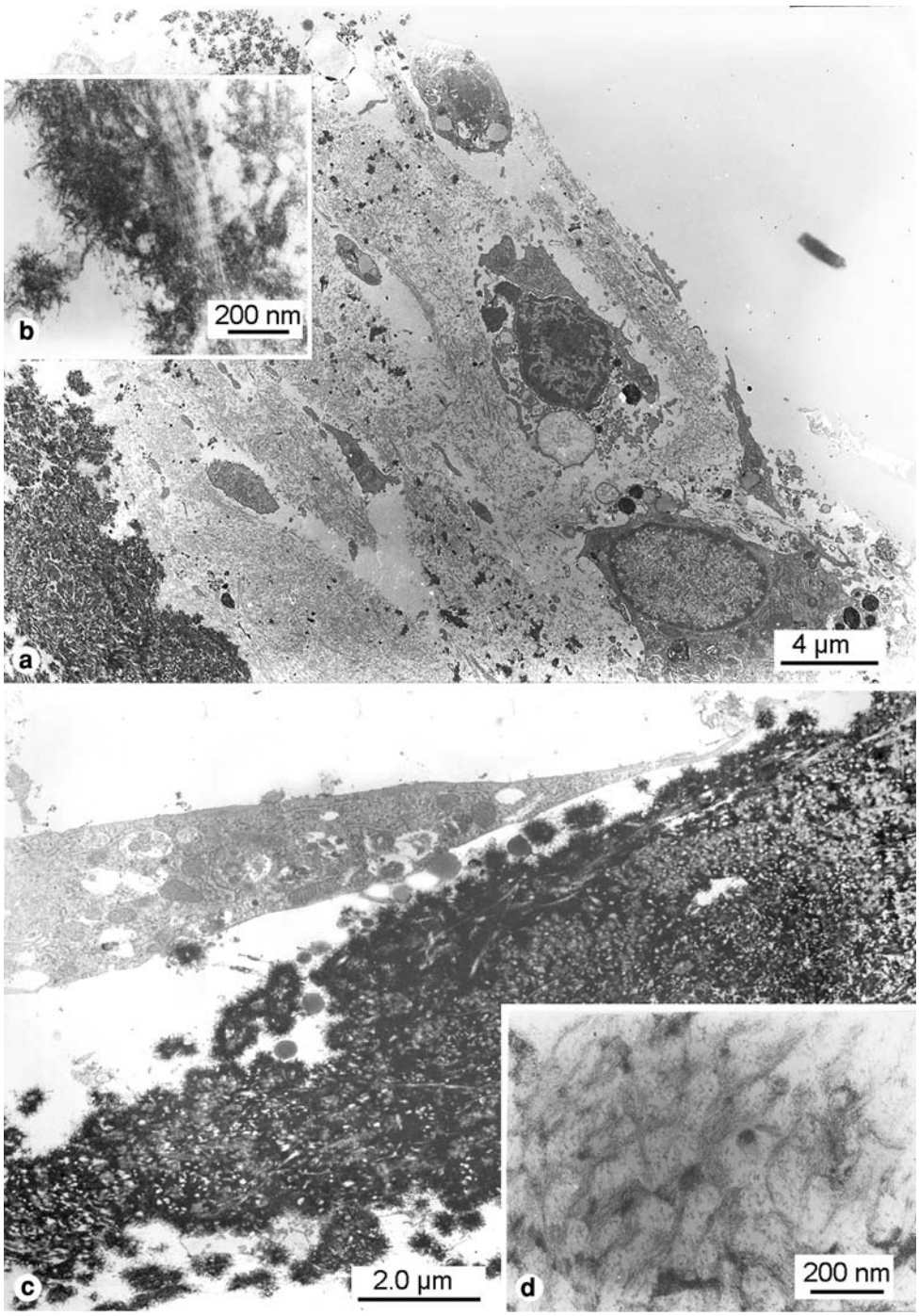

Fig. 5 TEM of LA/CL scaffold with apparent porosity of 70. (**a**, **c**) Bone/polymer interface; (**b**) extracellular matrix formation (collagen I fibers) and apatite crystals; (**d**) polymer with calcium phosphate crystals

sodium chloride [10, 16, 17, 20, 23]. Studies with sucrose [24–26] or gelatin [27, 28] as porogen are limited.

For injectable, in situ forming scaffolds, salt particulates as porogen cannot be used. The use of gelatin would have major benefits as gelatin melts at a temperature of 37°C and is biodegradable. To obtain highly interconnected scaffolds with maximal mechanical strength and lowest pore volume, gelatin and sucrose seemed promising. As demonstrated by SEM, scaffolds obtained with sodium chloride as porogen are not interconnected [8]. The pores of a scaffold are dictated by the leachable particles. Sodium chloride has a typical angular shape. The largest throat size can be produced when the face of one angular particle resides adjacent to another particle, however the chances of this configuration are very low in comparison to a particle corner abutting onto the corner, side or face of another particle. The use of angular particles cannot result in a uniform throat size throughout the scaffold [19]. Others describe that highly interconnected scaffolds with the salt-leaching technique can only be obtained when 70–90% salt

is added [10, 21]. On the contrary, Thomson et al. described that scaffolds with porosities higher than 58 could not be achieved with gelatin since swelling of the gelatin during the leaching process resulted in rupture of the foam structure [27].

To obtain scaffolds with the highest interconnectivity, highest mechanical strength and the lowest possible pore volume, the use of spherical and very irregular particles like gelatin, that also exhibit a better packing efficiency, is recommended [19]. For the same porosity, a better connectivity of the pores can be obtained with spherical gelatin in comparison to angular salt, which was also described by Suh et al. [28]. Sucrose particles are also cuboidal but more irregularities can be observed in comparison to sodium chloride resulting in a better interconnected pore morphology.

Moreover, it has previously been shown that fine grooves can be useful for controlling the direction of cellular migration over a surface [19]. Since a surface with roughness is important for cellular expression, the use of gelatin is a feasible alternative for the sodium chloride which surface is very smooth. According to Suh et al., scaffolds obtained by gelatin leaching showed better attachment of cells at the initial stage [28]. On the contrary, McGlohorn et al. described a higher initial attachment for scaffolds manufactured with sodium chloride rather than glucose [25].

Even in scaffolds with highly interconnected pores, the growth of mineralized tissue is limited to a penetration depth of approximately 200 μm. This is most likely due to a diffusion limitation effect (although the scaffold/cell constructs were cultured dynamically), and a physical obstruction from the mineralized tissue surrounding the scaffold [16]. For in vivo applications, it would be beneficial to mix the in situ photopolymerizable scaffold with osteoprogenitor cells or stem cells to induce bone formation in the center of the scaffold.

5 Conclusions

This study demonstrated that rat bone marrow cells can attach and differentiate when cultured on 3-D porous in situ photopolymerizable scaffolds based on D,L-lactide and ε-caprolactone. Pore volume, pore size and pore shape did not influence bone formation. Cellular infiltration was possible for scaffolds with high porosity [70] obtained by gelatin (250–355 μm) leaching. For scaffolds with lower porosity [60] and gelatin particle size 250–355 μm, no ingrowth occurred due to a polymer top layer, although cellular infiltration was possible when the gelatin particle size increased to 355–500 μm.

Pore shape did influence the pore morphology and interconnectivity of the scaffold. As spherical, irregular gelatin particles, in contrast to sodium chloride and to a lesser extent sucrose particles, are contributing to a better interconnected pore morphology at the same porosity [70], they are suitable as a porogen for in situ forming scaffolds.

Acknowledgements The work was supported by a fund of the Ghent University (GOA project 2001, No. 12050701). The authors thank L. Pieters and R. De Vos for technical assistance.

References

1. D.W. Hutmacher, T. Schantz, I. Zein, Ng.K. Woei, S. Hin Teoh, K. Cheng Tan, J. Biomed. Mater. Res. **55**(2), 203 (2001)
2. J.S. Temenoff, A.G. Mikos, Biomaterials **21**, 2405 (2000)
3. R.F. Storey, S.C. Warren, C.J. Allison, J.S. Wiggins, A.D. Puckett, Polymer **34**, 4365 (1993)
4. Z. Kucybala, M. Pietrak, J. Paczkowski, J.A. Linden, J.F. Rabek, Polymer **20**, 4585 (1996)
5. R.T. Thomson, M.J. Yaszmski, J.M. Powers, A.G. Mikos, J. Biomater. Sci. Polymer Ed. **7**, 23 (1995)
6. G. Jackers, Ontwikkeling van biodegradeerbare implantaten voor botweefselregeneratie. PhD thesis, 2002. Proefschrift voorgelegd tot het behalen van de graad: Doctor in de Wetenschappen, Scheikunde. Promotor: E. Schacht. Polymer Material Research Group, Krijgslaan 281 (S4), Ghent University, B-9000 Ghent, Belgium
7. E. Schacht, T. Gorski, G. Jackers, M. Cornelissen, H. Declercq, R. Verbeeck, N. Van den Vreken, F. Gasthuys, L. Vlaminck, Bone regeneration scaffolds prepared from crosslinkable biodegradable polymers. Abstract. 40th IUPAC Symposium on Macromolecules, Paris, 4–9 July 2004
8. T. Gorski, Preparation and evaluation of biodegradable composite scaffolds for bone tissue engineering. PhD thesis, 2006. Proefschrift voorgelegd tot het behalen van de graad: Doctor in de Wetenschappen, Scheikunde. Promotor: E. Schacht. Polymer material Research Group, Krijgslaan 281 (S4), Ghent University, B-9000 Ghent, Belgium
9. http://www.sigmaaldrich.com/catalog/search/ProductDetail/ALDRICH
10. A.G. Mikos, M.J. Thorsen, L.A. Czerwonka, Y. Bao, R. Langer, D.N. Winslow, J.P. Vacanti, Polymer **35**, 1068 (1994)
11. H.A. Declercq, R.M.H. Verbeeck, L.I.F.J.M. De Ridder, E.H. Schacht, M.J. Cornelissen, Biomaterials **26**, 4964 (2005)
12. H.A. Declercq, T.L. Gorski, M.J. Cornelissen, E.J. Schacht, J. Mater. Sci. Mater. Med. **17**, 113 (2006)
13. E.M. Noah, J. Chen, X. Jiao, I. Heschel, N. Pallua, Biomaterials **23**, 2855 (2002)
14. M. Radice, P. Brun, R. Cortivo, R. Scapinelli, C. Battaliard, G. Abatangelo, J. Biomed. Mater. Res. **50**, 101 (2000)
15. S.L. Ishaug, G.M. Crane, M.J. Miller, A.W. Yasko, M.J. Yaszemski, A.G. Mikos, J. Biomed. Mater. Res. **37**, 17 (1997)
16. S.L. Ishaug-Riley, G.M. Crane-Kruger, M.J. Yaszemski, A.G. Mikos, Biomaterials. **19**, 1405 (1998)
17. G. Ciapetti, L. Ambrosio, D. Savarino, E. Granchi, N. Cenni, N. Baldini, S. Pagani, S. Guizzardi, F. Causa, A. Giunti, Biomaterials. **24**, 3815 (2003)
18. J.M. Karp, M.S. Shoichet, J.E. Davies, J. Biomed. Mater. Res. **64A**, 388 (2003)
19. K.A. Gross, L.M. Rodriguez-Lorenzo, Biomaterials **25**, 4955 (2004)
20. J.A. Burdick, D. Frankel, W.S. Dernell, K.S. Anseth, Biomaterials **24**, 1613 (2003)
21. J.A. Burdick, R.F. Padera, J.V. Huang, K.S. Anseth, J. Biomed. Mater. Res. (Appl. Biomater.) **63**, 484 (2002)

22. E.L. Hedberg, C.K. Shih, J.J. Lemoine, M.D. Timmer, M.A.K. Liebschner, J.A. Jansen, A.G. Mikos, Biomaterials **26**, 3215 (2005)
23. K.G. Marra, J.W. Szem, P.N. Kumta, P.A. DiMilla, L.E. Weiss, J. Biomed. Mater. Res. **47**, 324 (1999)
24. C.E. Holy, M.S. Shoichet, J.E. Davies, J. Biomed. Mater. Res. **51**, 376 (2000)
25. J.B. McGlohorn, W.D. Holder Jr., L.W. Grimes, C.B. Thomas, K.J. Burg, Tissue Eng. **10**(3), 505 (2004)
26. A.J. Ahoo, T. Tirri J. Kukkonen, N. Strandberg, J. Rich, J. Seppälä, A. Yli-Urpo, J. Mater. Sci. Mat. Med. **15**, 1165 (2004)
27. R.C. Thomson, M.J. Yaszemski, J.M. Powers, A.G. Mikos, Biomaterials **19**(21), 1935 (1998)
28. S.W. Suh, J.Y. Shin, J. Kim, C.H. Beak, D.I. Kim, H. Kim, S.S. Jeon, I.W. Choo, ASAIO J. **48**(5), 460 (2002)